Ad Hoc Networks 24 (2015) 109–120

Contents lists available at ScienceDirect

Ad Hoc Networks

journal homepage: www.elsevier.com/locate/adhoc

Source delay in mobile ad hoc networks

Juntao Gao [a,*], Yulong Shen [b,c,1], Xiaohong Jiang [d], Jie Li [e]

[a] Graduate School of Information Science, Nara Institute of Science and Technology, 630-0192, Japan
[b] State Key Laboratory of Integrated Services Networks, Xidian University, Xian, Shaanxi 710071, PR China
[c] School of Computer Science and Technology, Xidian University, Xian, Shaanxi 710071, PR China
[d] School of Systems Information Science, Future University Hakodate, 116-2 Kamedanakano-cho, Hakodate, Hokkaido 041-8655, Japan
[e] Faculty of Engineering, Information and Systems, University of Tsukuba, Tsukuba Science City, Ibaraki 305-8573, Japan

ARTICLE INFO

Article history:
Received 21 November 2013
Received in revised form 6 March 2014
Accepted 9 August 2014
Available online 19 August 2014

Keywords:
MANETs
Packet dispatch
Source delay
Mean
Variance

ABSTRACT

Source delay, the time a packet experiences in its source node, serves as a fundamental quantity for delay performance analysis in networks. However, the source delay performance in highly dynamic mobile ad hoc networks (MANETs) is still largely unknown by now. This paper studies the source delay in MANETs based on a general packet dispatching scheme with dispatch limit f (PD-f for short), where a same packet will be dispatched out up to f times by its source node such that packet dispatching process can be flexibly controlled through a proper setting of f. We first apply the Quasi-Birth-and-Death (QBD) theory to develop a theoretical framework to capture the complex packet dispatching process in PD-f MANETs. With the help of the theoretical framework, we then derive the cumulative distribution function as well as mean and variance of the source delay in such networks. Finally, extensive simulation and theoretical results are provided to validate our source delay analysis and illustrate how source delay in MANETs is related to network parameters.

1. Introduction

Mobile ad hoc networks (MANETs) represent a class of self-configuring and infrastructureless networks with mobile nodes. As MANETs can be rapidly deployed, reconfigured and extended at low cost, they are highly appealing for a lot of critical applications, like disaster relief, emergency rescue, battle field communications, environment monitoring, etc. [1,2]. To facilitate the application of MANETs in providing delay guaranteed services in above applications, understanding the delay performance of these networks is of fundamental importance [3,4].

Source delay, the time a packet experiences in its source node, is an indispensable behavior in any network. Since the source delay is a delay quantity common to all MANETs, it serves as a fundamental quantity for delay performance analysis in MANETs. For MANETs where a packet is transmitted only once by its source node (through either unicast [5,6] or broadcast [7]), the source delay actually serves as a practical lower bound for and thus constitutes an essential part of overall delay in those networks. The source delay is also an indicator of packet lifetime, i.e., the maximum time a packet could stay in a network; in particular, it lower bounds the lifetime of a packet and thus serves as a crucial performance metric for MANETs with packet lifetime constraint.

Despite much research activity on delay performance analysis in MANETs (see Section 6 for related works), the source delay performance of such networks is still largely unknown by now. The source delay analysis in highly

* Corresponding author at:
E-mail addresses: jtgao@is.naist.jp (J. Gao), ylshen@mail.xidian.edu.cn (Y. Shen), jiang@fun.ac.jp (X. Jiang), lijie@cs.tsukuba.ac.jp (J. Li).
[1] Principal corresponding author.

http://dx.doi.org/10.1016/j.adhoc.2014.08.004
1570-8705/

dynamic MANETs is challenging, since it involves not only complex network dynamics like node mobility, but also issues related to medium contention, interference, packet generating and packet dispatching. This paper is devoted to a thorough study on the source delay in MANETs under the practical scenario of limited buffer size and also a general packet dispatching scheme with dispatch limit f (PD-f for short). With the PD-f scheme, a same packet will be dispatched out up to f times by its source node such that packet dispatching process can be flexibly controlled through a proper setting of f. The main contributions of this paper are summarized as follows.

- We first apply the Quasi-Birth-and-Death (QBD) theory to develop a theoretical framework to capture the complex packet dispatching process in a PD-f MANET. The theoretical framework is powerful in the sense it enables complex network dynamics to be incorporated into source delay analysis, like node mobility, medium contention, interference, packet transmitting and packet generating processes.
- With the help of the theoretical framework, we then derive the cumulative distribution function (CDF) as well as mean and variance of the source delay in the considered MANET. By setting $f = 1$ in a PD-f MANET, the corresponding source delay actually serves as a lower bound for overall delay.
- Extensive simulation results are provided to validate our theoretical framework and the source delay models. Based on the theoretical source delay models, we further demonstrate how source delay in MANETs is related to network parameters, such as packet dispatch limit, buffer size and packet dispatch probability.

The rest of this paper is organized as follows. Section 2 introduces preliminaries involved in this source delay study. A QBD based theoretical framework is developed to model the source delay in Section 3. We derive in Section 4 the CDF as well as mean and variance of the source delay. Simulation/numerical studies and the corresponding discussions are provided in Section 5. Finally, we introduce related works regarding delay performance analysis in MANETs in Section 6 and conclude the paper in Section 7.

2. Preliminaries

In this section, we introduce the basic system models, the Medium Access Control (MAC) protocol and the packet dispatching scheme involved in this study.

2.1. System models

2.1.1. Network model and mobility model

We consider a time slotted torus MANET of unit area. Similar to previous works, we assume that the network area is evenly partitioned into $m \times m$ cells as shown in Fig. 1a [8–11]. There are n mobile nodes in the network and they randomly move around following the Independent and Identically Distributed (IID) mobility model [6,12,13]. According to the IID mobility model, each node first moves into a randomly and uniformly selected cell at the beginning of a time slot and then stays in that cell during the whole time slot.

2.1.2. Communication model

We assume that all nodes transmit data through one common wireless channel, and each node (say S in Fig. 1a) employs the same transmission range $r = \sqrt{8}/m$ to cover 9 cells, including S's current cell and its 8 neighboring cells. To account for mutual interference and interruption among concurrent transmissions, the commonly used protocol model is adopted [10,12,14,15]. According to the protocol model, node i could successfully transmit to another node j if and only if $d_{ij} \leqslant r$ and for another simultaneously transmitting node $k \neq i,j$, $d_{kj} \geqslant (1 + \Delta) \cdot r$, where

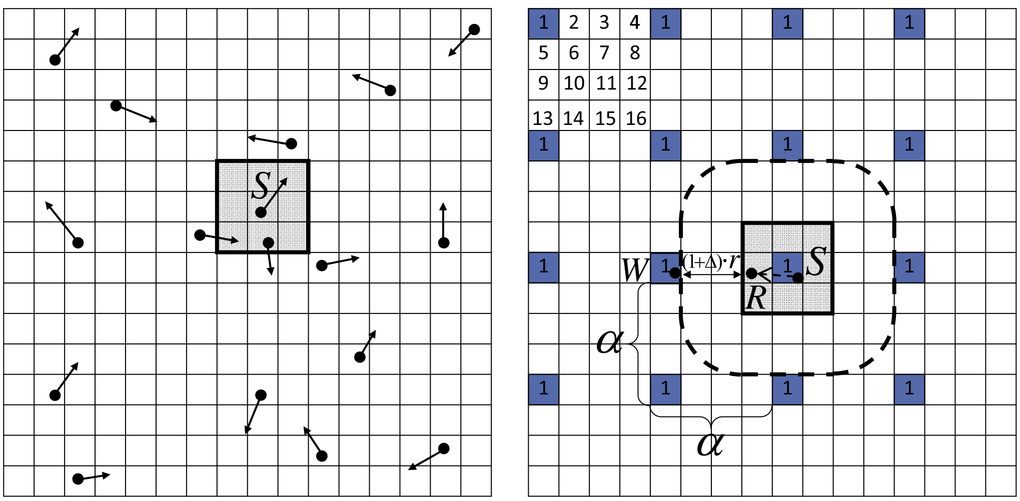

(a) A snapshot of a cell partitioned MANET. (b) Illustration of MAC-EC protocol.

Fig. 1. An example of a cell partitioned MANET with a MAC protocol.

d_{ij} denotes the Euclidean distance between node i and node j and $\Delta \geqslant 0$ is the guard factor to prevent interference. In a time slot, the data that can be transmitted during a successful transmission is normalized to one packet.

2.1.3. Traffic model

We consider the widely adopted permutation traffic model [10,12,13], where there are n distinct traffic flows in the network. Under such traffic model, each node acts as the source of one traffic flow and at the same time the destination of another traffic flow. The packet generating process in each source node is assumed to be a Bernoulli process, where a packet is generated by its source node with probability λ in a time slot [6]. We assume that each source node has a first-come-first-serve queue (called local-queue hereafter) with limited buffer size $M > 0$ to store its locally generated packets. Each locally generated packet in a source node will be inserted into the end of its local-queue if the queue is not full, and dropped otherwise.

2.2. MAC protocol

We adopt a commonly used MAC protocol based on the concept of Equivalent-Class to address wireless medium access issue in MANETs [10–12,15]. As illustrated in Fig. 1b that an Equivalent-Class (EC) consists of a group of cells with any two of them being separated by a horizontal and vertical distance of some integer multiple of $\alpha (1 \leqslant \alpha \leqslant m)$ cells. Under the EC-based MAC protocol (MAC–EC), the whole network cells are divided into α^2 ECs and ECs are then activated alternatively from time slot to time slot. We call cells in an activated EC as active cells, and only a node in an active cell could access the wireless channel and do packet transmission. If there are multiple nodes in an active cell, one of them is selected randomly to have a fair access to wireless channel.

To avoid interference among concurrent transmissions under the MAC–EC protocol, the parameter α should be set properly. Suppose a node (say S in Fig. 1b) in an active cell is transmitting to node R at the current time slot, and another node W in one adjacent active cell is also transmitting simultaneously. As required by the protocol model, the distance d_{WR} between W and R should satisfy the following condition to guarantee successful transmission from S to R,

$$d_{WR} \geqslant (1+\Delta)\cdot r. \tag{1}$$

Notice that $d_{WR} \geqslant (\alpha - 2)/m$, we have

$$(\alpha - 2)/m \geqslant (1+\Delta)\cdot r. \tag{2}$$

Since $\alpha \leqslant m$ and $r = \sqrt{8}/m$, α should be set as

$$\alpha = \min\left\{\lceil (1+\Delta)\sqrt{8} + 2 \rceil, m\right\}, \tag{3}$$

where the function $\lceil x \rceil$ returns the least integer value greater than or equal to x.

Remark 1. Notice that for a time slot and an active cell, the random selection of one node from multiple nodes to access wireless channel can be implemented based on a mechanism similar to DCF protocol [16,17]. At the beginning of the time slot, each node in the active cell first initiates a backoff timer with backoff period drawn uniformly from $[0, CW]$ (CW represents the contention window size), all nodes then begin to count down. The node whose timer reaches 0 first broadcasts a message claiming its access to the wireless channel, and all other nodes in the same active cell, after overhearing the broadcasted message, stop their timers and remain silent in the time slot.

2.3. PD-f scheme

Once a node (say S) got access to the wireless channel in a time slot, it then executes the PD-f scheme ($f \geqslant 1$) summarized in Algorithm 1 for packets dispatch.

Remark 2. The PD-f scheme is general and covers many widely used packet dispatching schemes as special cases, like the ones without packet redundancy [5,6,8] when $f = 1$ and only unicast transmission is allowed, the ones with controllable packet redundancy [12,16,18] when $f > 1$ and only unicast transmission is allowed, and the ones with uncontrollable packet redundancy [7,19] when $f \geqslant 1$ and broadcast transmission is allowed.

Algorithm 1. PD-f scheme.

if S has packets in its local-queue **then**
  S checks whether its destination D is within its transmission range;
  if D is within its transmission range **then**
    S transmits the head-of-line (HoL) packet in its local-queue to D;
      {source–destination transmission}
    S removes the HoL packet from its local-queue;
    S moves ahead the remaining packets in its local-queue;
  else
    With probability q ($0 < q < 1$), S dispatches the HoL packet;
    if S conducts packet dispatch **then**
      S dispatches the HoL packet for one time; {packet-dispatch transmission}
      if S has already dispatched the HoL packet for f times **then**
        S removes the HoL packet from its local-queue;
        S moves ahead the remaining packets in its local-queue;
      end if
    end if
  end if
else
  S remains idle;
end if

3. QBD-based theoretical framework

In this section, a QBD-based theoretical framework is developed to capture the packet dispatching process in a

PD-f MANET. This framework will help us to analyze source delay in Section 4.

3.1. QBD modeling

Due to the symmetry of source nodes, we only focus on a source node S in our analysis. We adopt a two-tuple $\mathbf{X}(t) = (L(t), J(t))$ to define the state of the local-queue in S at time slot t, where $L(t)$ denotes the number of packets in the local-queue at slot t and $J(t)$ denotes the number of packet dispatches that have been conducted for the current head-of-line packet by slot t, here $0 \leqslant L(t) \leqslant M, 0 \leqslant J(t) \leqslant f-1$ when $1 \leqslant L(t) \leqslant M$, and $J(t) = 0$ when $L(t) = 0$.

Suppose that the local-queue in S is at state (l,j) in the current time slot, all the possible state transitions that may happen at the next time slot are summarized in Fig. 2, where

- $I_0(t)$ is an indicator function, taking value of 1 if S conducts source–destination transmission in the current time slot, and taking value of 0 otherwise;
- $I_1(t)$ is an indicator function, taking value of 1 if S conducts packet-dispatch transmission in the current time slot, and taking value of 0 otherwise;
- $I_2(t)$ is an indicator function, taking value of 1 if S conducts neither source–destination nor packet-dispatch transmission in the current time slot, and taking value of 0 otherwise;
- $I_3(t)$ is an indicator function, taking value of 1 if S locally generates a packet in the current time slot, and taking value of 0 otherwise.

From Fig. 2 we can see that as time evolves, the state transitions of the local-queue in S form a two-dimensional QBD process [20]

$$\{\mathbf{X}(t),\ t = 0, 1, 2, \ldots\}, \tag{4}$$

on state space

$$\{\{(0,0)\} \cup \{(l,j)\}; 1 \leqslant l \leqslant M, 0 \leqslant j \leqslant f-1\}. \tag{5}$$

Based on the transition scenarios in Fig. 2, the overall transition diagram of above QBD process is illustrated in Fig. 3.

Remark 3. The QBD framework is powerful in the sense it enables main network dynamics to be captured, like the dynamics involved in the packet generating process and those involved in the source–destination and packet-dispatch transmissions (i.e., node mobility, medium contention, interference and packet transmitting).

3.2. Transition matrix and some basic results

As shown in Fig. 3 that there are in total $1 + M \cdot f$ two-tuple states for the local-queue in S. To construct the transition matrix of the QBD process, we arrange all these $1 + M \cdot f$ states in a left-to-right and top-to-down way as follows: $\{(0,0), (1,0), (1,1), \ldots, (1,f-1), (2,0), (2,1), \ldots, (2,f-1), \ldots, (M,0), \ldots, (M,f-1)\}$. Under such state

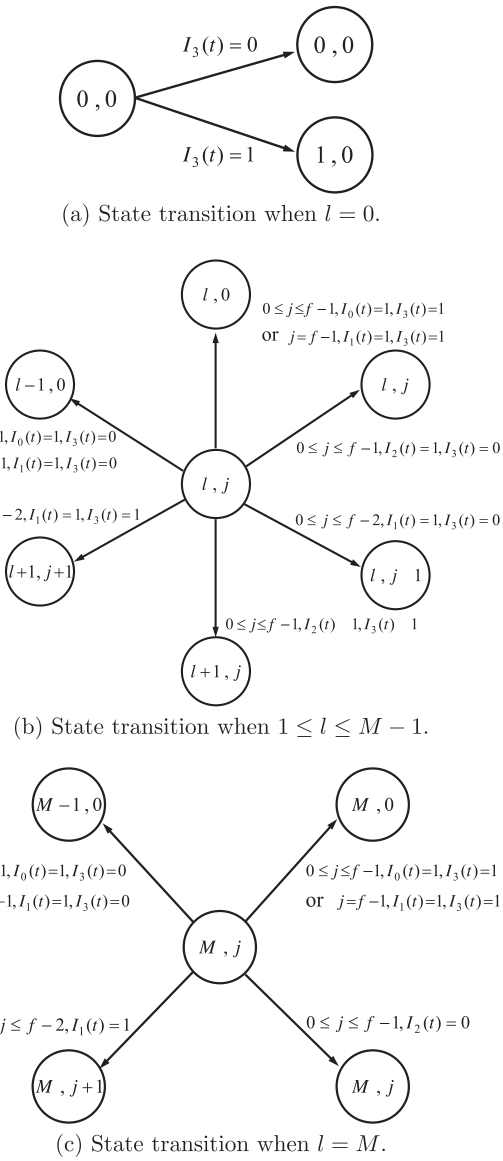

Fig. 2. State transitions from state (l,j) of the local-queue.

arrangement, the corresponding state transition matrix $\mathbf{P}$ of the QBD process can be determined as

$$\mathbf{P} = \begin{bmatrix} \mathbf{B_1} & \mathbf{B_0} & & & \\ \mathbf{B_2} & \mathbf{A_1} & \mathbf{A_0} & & \\ & \mathbf{A_2} & \ddots & \ddots & \\ & & \ddots & \mathbf{A_1} & \mathbf{A_0} \\ & & & \mathbf{A_2} & \mathbf{A_M} \end{bmatrix}, \tag{6}$$

where the corresponding sub-matrices in matrix $\mathbf{P}$ are defined as follows:

- $\mathbf{B_0}$: a matrix of size $1 \times f$, denoting the transition probabilities from $(0,0)$ to $(1,j), 0 \leqslant j \leqslant f-1$.
- $\mathbf{B_1}$: a matrix of size 1×1, denoting the transition probability from $(0,0)$ to $(0,0)$.

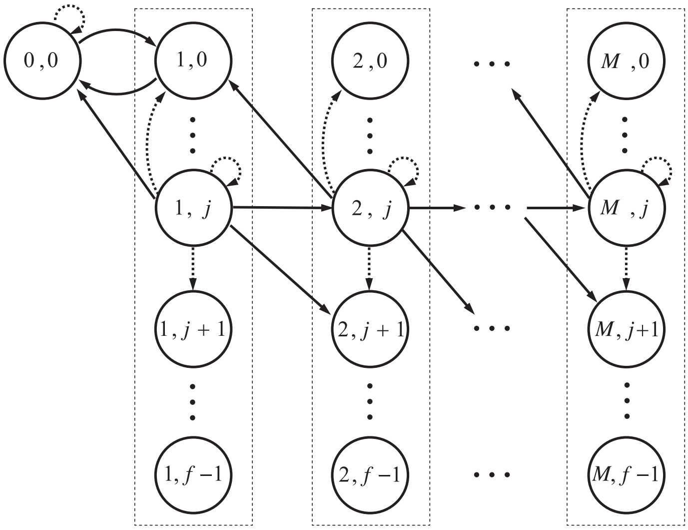

Fig. 3. State transition diagram for the QBD process of local-queue. For simplicity, only transitions from typical states (l,j) are illustrated for $1 \leqslant l \leqslant M$, while other transitions are the same as that shown in Fig. 2.

- $\mathbf{B_2}$: a matrix of size $f \times 1$, denoting the transition probabilities from $(1,j)$ to $(0,0), 0 \leqslant j \leqslant f-1$.
- $\mathbf{A_0}$: a matrix of size $f \times f$, denoting the transition probabilities from (l,j) to $(l+1,j'), 1 \leqslant l \leqslant M-1$, $0 \leqslant j,j' \leqslant f-1$.
- $\mathbf{A_1}$: a matrix of size $f \times f$, denoting the transition probabilities from (l,j) to $(l,j'), 1 \leqslant l \leqslant M-1, 0 \leqslant j,j' \leqslant f-1$.
- $\mathbf{A_2}$: a matrix of size $f \times f$, denoting the transition probabilities from (l,j) to $(l-1,j'), 2 \leqslant l \leqslant M, 0 \leqslant j,j' \leqslant f-1$.
- $\mathbf{A_M}$: a matrix of size $f \times f$, denoting the transition probabilities from (M,j) to $(M,j'), 0 \leqslant j,j' \leqslant f-1$.

Some basic probabilities involved in the above sub-matrices are summarized in the following Lemma.

Lemma 1. *For a given time slot, let p_0 be the probability that S conducts a source–destination transmission, let p_1 be the probability that S conducts a packet-dispatch transmission, and let p_2 be the probability that S conducts neither source–destination nor packet-dispatch transmission. Then, we have*

$$p_0 = \frac{1}{\alpha^2}\left\{\frac{9n-m^2}{n(n-1)} - \left(\frac{m^2-1}{m^2}\right)^{n-1}\frac{8n+1-m^2}{n(n-1)}\right\}, \tag{7}$$

$$p_1 = \frac{q(m^2-9)}{\alpha^2(n-1)}\left\{1 - \left(\frac{m^2-1}{m^2}\right)^{n-1}\right\}, \tag{8}$$

$$p_2 = 1 - p_0 - p_1. \tag{9}$$

Proof. See Appendix A for the proof. □

4. Source delay analysis

Based on the QBD-based theoretical framework developed above, this section conducts analysis on the source delay defined as follow.

Definition 1. In a PD-f MANET, the source delay U of a packet is defined as the time the packet experiences in its local-queue after it is inserted into the local-queue.

To analyze the source delay, we first examine the steady state distribution of the local-queue, based on which we then derive the CDF and mean/variance of the source delay.

4.1. State distribution of local-queue

We adopt a row vector $\boldsymbol{\pi}^*_\omega = [\pi^*_{\omega,0}\ \boldsymbol{\pi}^*_{\omega,1} \ldots \boldsymbol{\pi}^*_{\omega,M}]$ of size $1 + M \cdot f$ to denote the steady state distribution of the local-queue, here $\pi^*_{\omega,0}$ is a scalar value representing the probability that the local-queue is in the state $(0,0)$, while $\boldsymbol{\pi}^*_{\omega,l} = (\pi^*_{\omega,l,j})_{1\times f}$ is a sub-vector with $\pi^*_{\omega,l,j}$ being the probability that the local queue is in state $(l,j), 1 \leqslant l \leqslant M, 0 \leqslant j \leqslant f-1$.

For the analysis of source delay, we further define a row vector $\boldsymbol{\pi}^*_\Omega = [\pi^*_{\Omega,0}\ \boldsymbol{\pi}^*_{\Omega,1} \ldots \boldsymbol{\pi}^*_{\Omega,M}]$ of size $1 + M \cdot f$ to denote the conditional steady state distribution of the local-queue under the condition that a new packet has just been inserted into the local-queue, here $\pi^*_{\Omega,0}$ is a scalar value representing the probability that the local-queue is in the state $(0,0)$ under the above condition, while $\boldsymbol{\pi}^*_{\Omega,l} = (\pi^*_{\Omega,l,j})_{1\times f}$ is a sub-vector with $\pi^*_{\Omega,l,j}$ being the probability that the local queue is in state (l,j) under the above condition, $1 \leqslant l \leqslant M, 0 \leqslant j \leqslant f-1$. Regarding the evaluation of $\boldsymbol{\pi}^*_\Omega$, we have the following lemma.

Lemma 2. *In a PD-f MANET, its conditional steady local-queue state distribution $\boldsymbol{\pi}^*_\Omega$ is given by*

$$\boldsymbol{\pi}^*_\Omega = \frac{\boldsymbol{\pi}^*_\omega \mathbf{P_2}}{\lambda \boldsymbol{\pi}^*_\omega \mathbf{P_1} \mathbf{1}}, \tag{10}$$

where $\mathbf{1}$ is a column vector with all elements being 1. The matrix $\mathbf{P_1}$ in (10) is determined based on (6) by setting the corresponding sub-matrices as follows:

For $M = 1$,

$$\mathbf{B_0} = \mathbf{0}, \tag{11}$$
$$\mathbf{B_1} = [1], \tag{12}$$
$$\mathbf{B_2} = \mathbf{c}, \tag{13}$$
$$\mathbf{A_M} = \mathbf{0}. \tag{14}$$

For $M \geqslant 2$,

$$\mathbf{B_0} = \mathbf{0}, \tag{15}$$
$$\mathbf{B_1} = [1], \tag{16}$$
$$\mathbf{B_2} = \mathbf{c}, \tag{17}$$
$$\mathbf{A_0} = \mathbf{0}, \tag{18}$$
$$\mathbf{A_1} = \mathbf{Q}, \tag{19}$$
$$\mathbf{A_2} = \mathbf{c} \cdot \mathbf{r}, \tag{20}$$
$$\mathbf{A_M} = \mathbf{0}. \tag{21}$$

where $\mathbf{0}$ *is a matrix of proper size with all elements being* 0,

$$\mathbf{c} = [p_0 \quad \dots \quad p_0 \quad p_0 + p_1]^T, \tag{22}$$
$$\mathbf{r} = [1 \quad 0 \quad \dots \quad 0], \tag{23}$$
$$\mathbf{Q} = \begin{bmatrix} p_2 & p_1 & & & \\ & p_2 & p_1 & & \\ & & \ddots & \ddots & \\ & & & p_2 & p_1 \\ & & & & p_2 \end{bmatrix}. \tag{24}$$

The matrix $\mathbf{P_2}$ *in* (10) *is also determined based on* (6) *by setting the corresponding sub-matrices as follows:*

For $M = 1$,

$$\mathbf{B_0} = [\lambda \quad 0 \quad \dots \quad 0], \tag{25}$$
$$\mathbf{B_1} = [0], \tag{26}$$
$$\mathbf{B_2} = \mathbf{0}, \tag{27}$$
$$\mathbf{A_M} = \lambda \mathbf{c} \cdot \mathbf{r}. \tag{28}$$

For $M \geqslant 2$,

$$\mathbf{B_0} = [\lambda \quad 0 \quad \dots \quad 0], \tag{29}$$
$$\mathbf{B_1} = [0], \tag{30}$$
$$\mathbf{B_2} = \mathbf{0}, \tag{31}$$
$$\mathbf{A_0} = \lambda \mathbf{Q}, \tag{32}$$
$$\mathbf{A_1} = \lambda \mathbf{c} \cdot \mathbf{r}, \tag{33}$$
$$\mathbf{A_2} = \mathbf{0}, \tag{34}$$
$$\mathbf{A_M} = \lambda \mathbf{c} \cdot \mathbf{r}. \tag{35}$$

Proof. See Appendix B for the proof. □

The result in (10) indicates that for the evaluation of $\boldsymbol{\pi}^*_\Omega$, we still need to determine the steady state distribution $\boldsymbol{\pi}^*_\omega$ of the local-queue.

Lemma 3. *In a PD-f MANET, its steady state distribution* $\boldsymbol{\pi}^*_\omega$ *of the local-queue is determined as follows:*

For $M = 1$,

$$\pi^*_{\omega,0} = \pi^*_{\omega,0}\mathbf{B_1} + \boldsymbol{\pi}^*_{\omega,1}\mathbf{B_2}, \tag{36}$$
$$\boldsymbol{\pi}^*_{\omega,1} = \pi^*_{\omega,0}\mathbf{B_0} + \boldsymbol{\pi}^*_{\omega,1}\mathbf{A_M}, \tag{37}$$
$$\boldsymbol{\pi}^*_{\omega} \cdot \mathbf{1} = 1. \tag{38}$$

For $M = 2$,

$$\pi^*_{\omega,0} = \pi^*_{\omega,0}\mathbf{B_1} + \boldsymbol{\pi}^*_{\omega,1}\mathbf{B_2}, \tag{39}$$
$$\boldsymbol{\pi}^*_{\omega,1} = \pi^*_{\omega,0}\mathbf{B_0} + \boldsymbol{\pi}^*_{\omega,1}\mathbf{A_1} + \boldsymbol{\pi}^*_{\omega,2}\mathbf{A_2}, \tag{40}$$
$$\boldsymbol{\pi}^*_{\omega,2} = \boldsymbol{\pi}^*_{\omega,1}\mathbf{A_0} + \boldsymbol{\pi}^*_{\omega,2}\mathbf{A_M}, \tag{41}$$
$$\boldsymbol{\pi}^*_{\omega} \cdot \mathbf{1} = 1. \tag{42}$$

For $M \geqslant 3$,

$$[\pi^*_{\omega,0}, \boldsymbol{\pi}^*_{\omega,1}] = [\pi^*_{\omega,0}, \boldsymbol{\pi}^*_{\omega,1}] \begin{bmatrix} \mathbf{B_1} & \mathbf{B_0} \\ \mathbf{B_2} & \mathbf{A_1} + \mathbf{R}\mathbf{A_2} \end{bmatrix}, \tag{43}$$
$$\boldsymbol{\pi}^*_{\omega,i} = \boldsymbol{\pi}^*_{\omega,1}\mathbf{R}^{i-1}, \quad 2 \leqslant i \leqslant M-1, \tag{44}$$
$$\boldsymbol{\pi}^*_{\omega,M} = \boldsymbol{\pi}^*_{\omega,1}\mathbf{R}^{M-2}\mathbf{R_M}, \tag{45}$$
$$\boldsymbol{\pi}^*_{\omega} \cdot \mathbf{1} = 1, \tag{46}$$

where

$$\mathbf{B_0} = [\lambda \quad 0 \quad \dots \quad 0], \tag{47}$$
$$\mathbf{B_1} = [1-\lambda], \tag{48}$$
$$\mathbf{B_2} = (1-\lambda)\mathbf{c}, \tag{49}$$
$$\mathbf{A_0} = \lambda \mathbf{Q}, \tag{50}$$
$$\mathbf{A_1} = (1-\lambda)\mathbf{Q} + \lambda \mathbf{c} \cdot \mathbf{r}, \tag{51}$$
$$\mathbf{A_2} = (1-\lambda)\mathbf{c} \cdot \mathbf{r}, \tag{52}$$
$$\mathbf{A_M} = \mathbf{A_1} + \mathbf{A_0}, \tag{53}$$
$$\mathbf{R} = \mathbf{A_0}[\mathbf{I} - \mathbf{A_1} - \mathbf{A_0} \cdot \mathbf{1} \cdot \mathbf{r}]^{-1}, \tag{54}$$
$$\mathbf{R_M} = \mathbf{A_0}[\mathbf{I} - \mathbf{A_M}]^{-1}, \tag{55}$$

here $\mathbf{c}$, $\mathbf{r}$ *and* $\mathbf{Q}$ *are given in* (22)–(24), *respectively;* $\mathbf{I}$ *is an identity matrix of size* $f \times f$, *and* $\mathbf{1}$ *is a column vector of proper size with all elements being 1.*

Proof. See Appendix C for the proof. □

4.2. CDF, mean and variance of source delay

Based on the conditional steady state distribution $\boldsymbol{\pi}^*_\Omega$ of the local-queue, we are now ready to derive the CDF as well as mean and variance of the source delay, as summarized in the following theorem.

Theorem 1. *In a PD-f MANET, the probability mass function* $Pr\{U = u\}$, *CDF* $Pr\{U \leqslant u\}$, *mean* $\overline{U}$ *and variance* σ_U^2 *of the source delay U of a packet are given by*

$$Pr\{U = u\} = \boldsymbol{\pi}^-_\Omega \mathbf{T}^{u-1}\mathbf{c}^+, \quad u \geqslant 1, \tag{56}$$
$$Pr\{U \leqslant u\} = 1 - \boldsymbol{\pi}^-_\Omega \mathbf{T}^{u}\mathbf{1}, \quad u \geqslant 0, \tag{57}$$
$$\overline{U} = \boldsymbol{\pi}^-_\Omega (\mathbf{I} - \mathbf{T})^{-2}\mathbf{c}^+, \tag{58}$$
$$\sigma_U^2 = \boldsymbol{\pi}^-_\Omega (\mathbf{I} + \mathbf{T})(\mathbf{I} - \mathbf{T})^{-3}\mathbf{c}^+ - \overline{U}^2, \tag{59}$$

where $\boldsymbol{\pi}^-_\Omega = [\boldsymbol{\pi}^*_{\Omega,1} \ \boldsymbol{\pi}^*_{\Omega,2} \dots \boldsymbol{\pi}^*_{\Omega,M}]$ *is a sub vector of* $\boldsymbol{\pi}^*_\Omega$, $\mathbf{c}^+$ *is a column vector of size* $M \cdot f$ *and* $\mathbf{T}$ *is a matrix of size* $(M \cdot f) \times (M \cdot f)$ *determined as follows:*

For $M = 1$,

$$\mathbf{c}^+ = \mathbf{c}, \tag{60}$$
$$\mathbf{T} = \mathbf{Q}. \tag{61}$$

For $M \geqslant 2$,

$$\mathbf{c}^{+} = [\mathbf{c} \quad 0 \quad \ldots \quad 0]^{T}, \tag{62}$$

$$\mathbf{T} = \begin{bmatrix} \mathbf{A_1} & \mathbf{A_0} & & & \\ \mathbf{A_2} & \mathbf{A_1} & \mathbf{A_0} & & \\ & \ddots & \ddots & \ddots & \\ & & \mathbf{A_2} & \mathbf{A_1} & \mathbf{A_0} \\ & & & \mathbf{A_2} & \mathbf{A_M} \end{bmatrix}, \tag{63}$$

where

$$\mathbf{A_0} = \mathbf{0}, \tag{64}$$

$$\mathbf{A_1} = \mathbf{Q}, \tag{65}$$

$$\mathbf{A_2} = \mathbf{c} \cdot \mathbf{r}, \tag{66}$$

$$\mathbf{A_M} = \mathbf{Q}, \tag{67}$$

here $\mathbf{c}$, $\mathbf{r}$ *and* $\mathbf{Q}$ *are given in (22)–(24), respectively, and* $\mathbf{0}$ *is a matrix of proper size with all elements being 0.*

Proof. See Appendix D for the proof. □

Remark 4. As a packet will be dispatched out by its source node for at least one time, the source delay under $f = 1$ actually serves as a lower bound for overall delay in PD-f MANETs.

5. Numerical results

In this section, we first provide simulation results to validate the efficiency of our QBD-based theoretical framework and source delay models, and then illustrate how source delay in a PD-f MANET is related to network parameters.

5.1. Source delay validation

To validate the theoretical framework and source delay models, a customized C++ simulator was developed to simulate the packet generating and dispatching processes in PD-f MANETs [21], in which network parameters, such as the number of network nodes n, network partition parameter m, local-queue buffer size M, packet dispatch limit f, packet dispatch probability q and packet generating probability λ, can be flexibly adjusted to simulate source delay performance under various network scenarios. Based on the simulator, extensive simulations have been conducted to validate our QBD-based source delay models. For three typical network scenarios of $n = 100$ (small network), $n = 200$ (medium network) and $n = 400$ (large network) with $m = 8$, $M = 7$, $f = 2$, $q = 0.4$ and $\lambda = 0.001$, the corresponding simulation/theoretical results on the CDFs of source delay are summarized in Fig. 4.

We can see from Fig. 4 that for all three network scenarios considered here, the theoretical results on the CDF of source delay match nicely with the corresponding simulated ones, indicating that our QBD-based theoretical framework is highly efficient in modeling the source delay behaviors of PD-f MANETs. We can also see from Fig. 4 that the source delay in a small network (e.g. $n = 100$ here) is very likely smaller than that of a large network (e.g. $n = 200$ or $n = 400$ here). This is because that for a given network area and a fixed partition parameter m, as net-

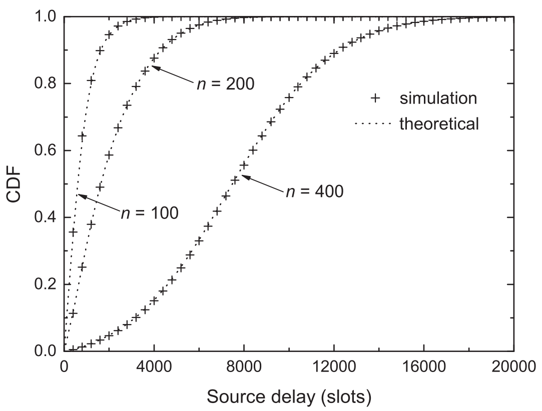

Fig. 4. The simulation and theoretical results on cumulative distribution function (CDF) of source delay.

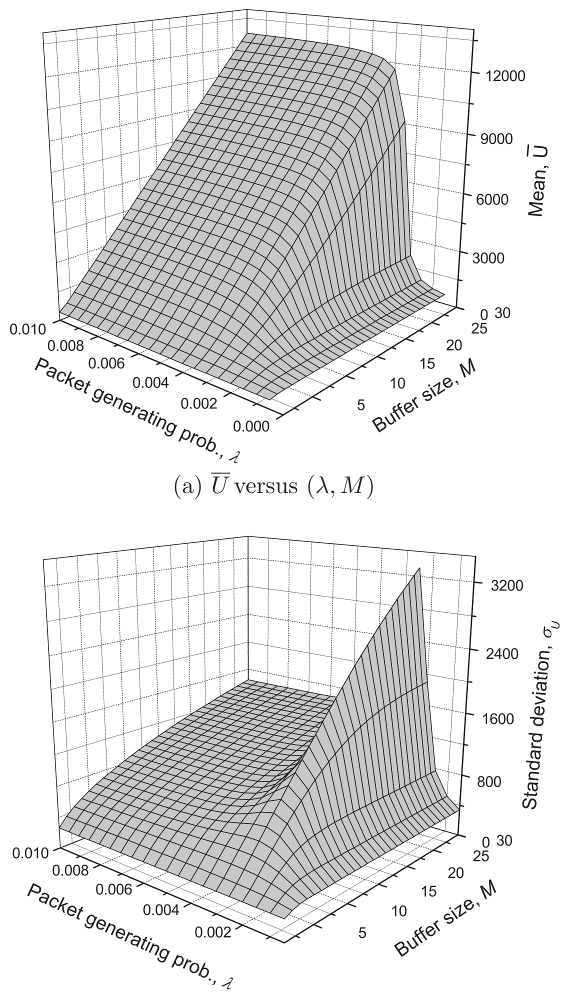

Fig. 5. Source delay performance versus packet generating probability λ and local-queue buffer size M.

work size in terms of n decreases the channel contention becomes less severe and thus each source node has more chances to conduct packet dispatch, leading to a shorter source delay one packet experiences in its source node.

5.2. Source delay illustrations

With our QBD-based theoretical framework, we then illustrate how source delay performance, in terms of its mean $\overline{U}$ and standard deviation $\sigma_U = \sqrt{\sigma_U^2}$, is related to some main network parameters like packet generating probability λ, local-queue buffer size M, packet dispatch limit f and packet dispatch probability q.

We first illustrate in Fig. 5 how $\overline{U}$ and σ_U vary with λ and M for a network scenario of $n = 200$, $m = 16$, $q = 0.6$ and $f = 3$. We see from Fig. 5a that for any given M, $\overline{U}$ first increases as λ increases until λ reaches some threshold value and then $\overline{U}$ remains almost a constant as λ increases further beyond that threshold. On the other hand, for a given $\lambda \in [0.0005, 0.002]$, as M increases $\overline{U}$ first increases and then remains constant, while for a given $\lambda \in [0.002, 0.01]$, $\overline{U}$ always increases as M increases. Regarding the standard deviation σ_U of source delay, we see from Fig. 5b that for given M, as λ increases from 0.0005 to 0.01 σ_U first increases sharply to a peak value, then decreases sharply, and finally converges to a constant. It is interesting to see that the peak values of σ_U under different settings of M are all achieved at the same $\lambda = 0.0025$. The results in Fig. 5b further indicate that for fixed λ, as M increases σ_U always first increases and then gradually converges to a constant.

We then illustrate in Fig. 6 how $\overline{U}$ and σ_U vary with packet dispatch parameters q and f under the network scenario of $n = 300$, $m = 16$, $M = 7$ and $\lambda = 0.002$. From Fig. 6a and b we can see that although both $\overline{U}$ and σ_U always decrease as q increases for a fixed f, their variations with q change dramatically with the setting of f. On the other hand, for a given $q \in [0.05, 0.2]$, as f increases both $\overline{U}$ and σ_U first increase and then tend to a constant, while for a given $q \in [0.2, ,1.0]$, both $\overline{U}$ and σ_U always monotonically increase as f increases.

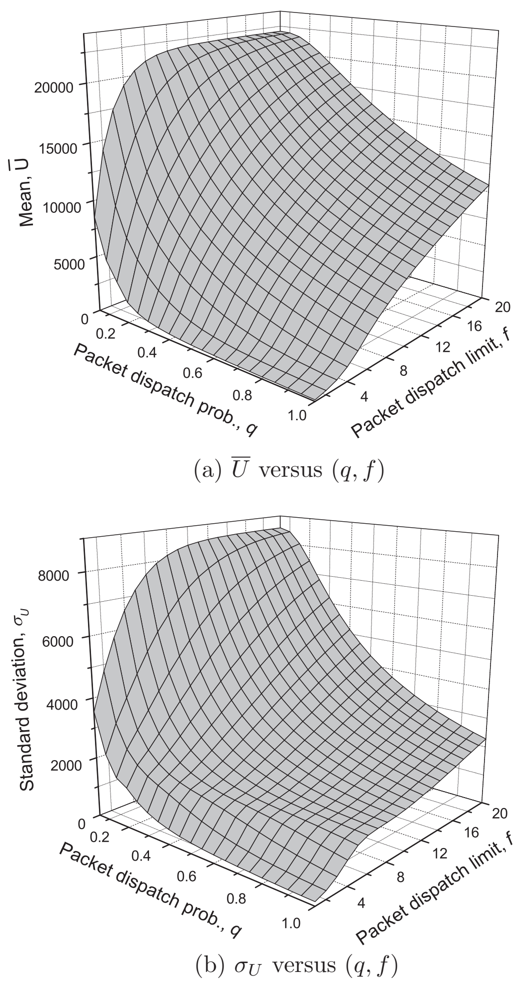

Fig. 6. Source delay performance versus packet dispatch probability q and packet dispatch limit f.

6. Related works

A substantial amount of works have been devoted to the study of delay performance in MANETs, which can be roughly divided into partial delay study and overall delay study.

6.1. Partial delay study

The available works on partial delay study in MANETs mainly focus on the delivery delay analysis [12,18,22–27] and local delay analysis [28–30], which constitutes only a part of the overall packet delay.

The delivery delay, defined as the time it takes a packet to reach its destination after its source starts to deliver it, has been extensively studied in the literature. For sparse MANETs without channel contentions, the Laplace–Stieltjes transform of delivery delay was studied in [25]; later, by imposing lifetime constraints on packets, the cumulative distribution function and n-th order moment of delivery delay were examined in [22,26]; the delivery delay was also studied in [18,23,27] under different assumptions on inter-meeting time among mobile nodes. For more general MANETs with channel contentions, closed-form results on mean and variance of delivery delay were recently reported in [12]. Regarding the local delay, i.e. the time it takes a node to successfully transmit a packet to its next-hop receiver, it was reported in [28] that some MANETs may suffer from a large and even infinite local delay. The work [29] indicates that the power control serves as a very efficient approach to ensuring a finite local delay in MANETs. It was further reported in [30] that by properly exploiting node mobility in MANETs it is possible for us to reduce local delay there.

6.2. Overall delay analysis

Overall delay (also called end-to-end delay), defined as the time it takes a packet to reach its destination after it is generated at its source, has also been extensively studied in the literature. For MANETs with two-hop relay routing, closed-form upper bounds on expected overall delay were derived in [6,16]. For MANETs with two-hop relay routing and its variants, approximation results on expected overall delay were presented in [13,31]. For MANETs with multi-hop relay routing and simple linear network topology, analytic results on expected overall delay and algorithm for computing expected overall delay were reported in [32,33] when the source there has only one packet to be transmitted to its destination; along this line, upper bounds on the cumulative distribution function of overall delay and approximations to Laplace–Stieltjes Transform of overall delay were further explored in [34–36] when the source has multiple packets to be transmitted to its destination. For MANETs with multi-hop relay routing and non-linear network topology, some initial results on the approximation of expected overall delay can be found in [37]. Rather than studying upper bounds and approximations on overall delay, some recent works explored the exact overall delay and showed that it is possible to derive the exact results on overall delay for MANETs under some special two-hop relay routings [6,7].

7. Conclusion

This paper conducted a thorough study on the source delay in MANETs, a new and fundamental delay metric for such networks. A QBD-based theoretical framework was developed to model the source delay behaviors under a general packet dispatching scheme, based on which the cumulative distribution function as well as the mean and variance of source delay were derived. As validated through extensive simulation results, our QBD-based framework is highly efficient in modeling the source delay performance in MANETs. Numerical results were also provided to illustrate how source delay is related to and thus can be controlled by some key network parameters, like local-queue buffer size, packet dispatch limit, and packet dispatch probability.

Notice that we studied the source delay in MANETs under the independent and identically distributed mobility model, an interesting future work is to extend our theoretical model to analyze source delay for MANETs under other popular mobility models, like the random walk and random waypoint mobility models. Note also that the theoretical framework developed in this paper concerns only source delay modeling, so another future research direction is to generalize our theoretical framework to model the overall delay in MANETs.

Acknowledgment

This work is partially supported by JSPS Grant (B) 24300026.

Appendix A. Proof of Lemma 1

The proof process is similar to that in [13,16]. We omit the proof details here and just outline the main idea of the proof. To derive the probability p_0 (resp. p_1), we first divide the event that S conducts a source–destination transmission (resp. packet-dispatch transmission) in a time slot into following sub-events: (1) S moves into an active cell in the time slot according to the IID mobility model; (2) S successfully accesses the wireless channel after fair contention according to the MAC–EC protocol; (3) S selects to conduct source–destination transmission (resp. packet-dispatch transmission) according to the PD-f scheme. We can then derive probability p_0 (resp. p_1) by combining the probabilities of these sub-events.

Appendix B. Proof of Lemma 2

To derive the conditional steady state distribution $\boldsymbol{\pi}^*_\Omega$ of the local-queue under the condition that a packet has just been inserted into the queue, we first study its corresponding transient state distribution $\boldsymbol{\pi}_\Omega(t+1)$ at time slot $t+1$.

Similar to the definition of $\boldsymbol{\pi}^*_\Omega$, we can see that the $(2+(l-1)f+j)$-th entry of row vector $\boldsymbol{\pi}_\Omega(t+1)$, denoted by $[\boldsymbol{\pi}_\Omega(t+1)]_{2+(l-1)f+j}$ here, corresponds to the probability that the local-queue is in state $\mathbf{X}(t+1)=(l,j)$ in time slot $t+1$ under the condition that a packet has just been inserted into the local-queue in time slot t, $1 \leqslant l \leqslant M$, $0 \leqslant j \leqslant f-1$. The basic state transition from $\mathbf{X}(t)$ to $\mathbf{X}(t+1)$ is illustrated in Fig. B.7, where $I_0(t)$ through $I_3(t)$ are indicator functions defined in Section 3.1, and $I_4(t)$ is a new indicator function, taking value of 1 if the local-queue is not full in time slot t (i.e. the local-queue is in some state in $\{\{(0,0)\}\cup\{(l,j)\};\ 1\leqslant l\leqslant M-1,\ 0\leqslant j\leqslant f-1\}$), and taking value of 0 otherwise.

From Fig. B.7 we can see that $[\boldsymbol{\pi}_\Omega(t+1)]_{2+(l-1)f+j}$ is evaluated as

$$[\boldsymbol{\pi}_\Omega(t+1)]_{2+(l-1)f+j} \tag{B.1}$$
$$= Pr\{\mathbf{X}(t+1)=(l,j)|I_4(t)=1, I_3(t)=1\} \tag{B.2}$$
$$= \frac{Pr\{I_4(t)=1, I_3(t)=1, \mathbf{X}(t+1)=(l,j)\}}{Pr\{I_4(t)=1, I_3(t)=1\}} \tag{B.3}$$
$$= \frac{Pr\{I_4(t)=1, I_3(t)=1, \mathbf{X}(t+1)=(l,j)\}}{\lambda\cdot Pr\{I_4(t)=1\}}, \tag{B.4}$$

where (B.4) follows because the packet generating process is a Bernoulli process independent of the state of the local-queue.

For the probability $Pr\{I_4(t)=1\}$ in (B.4), we have

$$Pr\{I_4(t)=1\} \tag{B.5}$$
$$= \sum_{(l',j')} Pr\{I_4(t)=1, \mathbf{X}(t)=(l',j')\} \tag{B.6}$$
$$= \sum_{(l',j')} Pr\{\mathbf{X}(t)=(l',j')\}Pr\{I_4(t)=1|\mathbf{X}(t)=(l',j')\} \tag{B.7}$$

where $Pr\{I_4(t)=1|\mathbf{X}(t)=(l',\ j')\}$ is actually the transition probability from state $\mathbf{X}(t)=(l',\ j')$ to states in

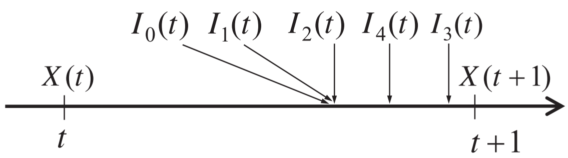

Fig. B.7. Illustration for state transition from $\mathbf{X}(t)$ to $\mathbf{X}(t+1)$ during time slot $[t, t+1)$.

$\{\{(0,0)\}\cup\{(l,j)\};\ 1\leqslant l\leqslant M-1,\ 0\leqslant j\leqslant f-1\}$. The matrix $\mathbf{P_1}$ of such transition probabilities can be determined based on (6) by setting the corresponding sub-matrices according to (11)–(21). With matrix $\mathbf{P_1}$ and (B.7), we have

$$Pr\{I_4(t)=1\}=\boldsymbol{\pi}_\omega(t)\cdot\mathbf{P_1}\cdot\mathbf{1}, \tag{B.8}$$

where $\boldsymbol{\pi}_\omega(t)=(\boldsymbol{\pi}_{\omega,l,j}(t))_{1\times M\cdot f}$ with $\boldsymbol{\pi}_{\omega,l,j}(t)$ being the probability $Pr\{\mathbf{X}(t)=(l',j')\}$.

For the numerator of (B.4), we have

$$Pr\{I_4(t)=1,\ I_3(t)=1,\ \mathbf{X}(t+1)=(l,j)\} \tag{B.9}$$
$$=\sum_{(l',j')}Pr\{\mathbf{X}(t)=(l',j'),I_4(t)=1,I_3(t)=1,\mathbf{X}(t+1)=(l,j)\} \tag{B.10}$$
$$=\sum_{(l',j')}Pr\{\mathbf{X}(t)=(l',j')\}$$
$$\cdot Pr\{I_4(t)=1,I_3(t)=1,\mathbf{X}(t+1)=(l,j)|\mathbf{X}(t)=(l',j')\}, \tag{B.11}$$

where $Pr\{I_4(t)=1,\ I_3(t)=1,\ \mathbf{X}(t+1)=(l,j)|\mathbf{X}(t)=(l',j')\}$ represents the transition probability from state $\mathbf{X}(t)=(l',j')$ to state $\mathbf{X}(t+1)=(l,j)$, when events $\{I_4(t)=1\}$ and $\{I_3(t)=1\}$ also happen simultaneously. The matrix $\mathbf{P_2}$ of such transition probabilities is determined based on (6) by setting the corresponding sub-matrices according to (25)–(34). With matrix $\mathbf{P_2}$ and (B.11), we have

$$Pr\{I_4(t)=1,I_3(t)=1,\mathbf{X}(t+1)=(l,j)\}$$
$$=[\boldsymbol{\pi}_\omega(t)\mathbf{P_2}]_{2+(l-1)f+j}. \tag{B.12}$$

After substituting (B.8) and (B.12) into (B.4), we get

$$[\boldsymbol{\pi}_\Omega(t+1)]_{2+(l-1)f+j}=\frac{[\boldsymbol{\pi}_\omega(t)\mathbf{P_2}]_{2+(l-1)f+j}}{\lambda\boldsymbol{\pi}_\omega(t)\mathbf{P_1}\mathbf{1}}. \tag{B.13}$$

Thus, in vector form

$$\boldsymbol{\pi}_\Omega(t+1)=\frac{\boldsymbol{\pi}_\omega(t)\mathbf{P_2}}{\lambda\boldsymbol{\pi}_\omega(t)\mathbf{P_1}\mathbf{1}}. \tag{B.14}$$

Taking limits on both sides of (B.14), we get the steady state distribution $\boldsymbol{\pi}^*_\Omega$ as

$$\boldsymbol{\pi}^*_\Omega=\lim_{t\to\infty}\boldsymbol{\pi}_\Omega(t+1) \tag{B.15}$$
$$=\lim_{t\to\infty}\frac{\boldsymbol{\pi}_\omega(t)\mathbf{P_2}}{\lambda\boldsymbol{\pi}_\omega(t)\mathbf{P_1}\mathbf{1}} \tag{B.16}$$
$$=\frac{\boldsymbol{\pi}^*_\omega\mathbf{P_2}}{\lambda\boldsymbol{\pi}^*_\omega\mathbf{P_1}\mathbf{1}}, \tag{B.17}$$

where

$$\boldsymbol{\pi}^*_\omega=\lim_{t\to\infty}\boldsymbol{\pi}_\omega(t). \tag{B.18}$$

This completes the proof of Lemma 2.

Appendix C. Proof of Lemma 3

Recall that as time evolves, the state transitions of the local-queue form a QBD process shown in Fig. 3. From Fig. 3, we can see that the QBD process has finite states and all states communicate with other states, so the Markov chain is recurrent. We also see from Fig. 3 that every state could transition to itself, indicating that the Markov chain is aperiodic. Thus, the concerned QBD process is an ergodic Markov chain and thus has a unique limit state distribution $\boldsymbol{\pi}^*_\omega$ defined in (B.18).

Notice that $\boldsymbol{\pi}^*_\omega$ must satisfy the following equation

$$\boldsymbol{\pi}^*_\omega=\boldsymbol{\pi}^*_\omega\mathbf{P_0}, \tag{C.1}$$

where $\mathbf{P_0}$ is the transition matrix of the QBD process, which can be determined based on (6) by setting the corresponding sub-matrices according to (47)–(53). In particular, for $M=1$ and $M=2$, the transition matrix $\mathbf{P_0}$ is given by the following (C.2) and (C.3), respectively.

$$\mathbf{P_0}=\begin{bmatrix}\mathbf{B_1} & \mathbf{B_0}\\ \mathbf{B_2} & \mathbf{A_M}\end{bmatrix}, \tag{C.2}$$

$$\mathbf{P_0}=\begin{bmatrix}\mathbf{B_1} & \mathbf{B_0} & \\ \mathbf{B_2} & \mathbf{A_1} & \mathbf{A_0}\\ & \mathbf{A_2} & \mathbf{A_M}\end{bmatrix}. \tag{C.3}$$

Thus, under the cases of $M=1$ and $M=2$, $\boldsymbol{\pi}^*_\omega$ could be easily calculated by Eqs. (36)–(42), respectively. Due to the special structure of the matrix $\mathbf{A_2}$, which is the product of a column vector $\mathbf{c}$ by a row vector $\mathbf{r}$ [20], $\boldsymbol{\pi}^*_\omega$ under the case $M\geqslant 3$ could be calculated by Eqs. (43)–(46).

Appendix D. Proof of Theorem 1

Suppose that the local-queue is in some state according to the steady state distribution $\boldsymbol{\pi}^*_\Omega$, then the source delay of a packet (say Z) is independent of the packet generating process after Z is inserted into the local-queue and is also independent of the state transitions of the local-queue after Z is removed from the local-queue. Such independence makes it possible to construct a simplified QBD process to study the source delay of packet Z, in which new packets generated after packet Z are ignored, and once Z is removed from the local-queue (or equivalently the local-queue transits to state $(0,0)$), the local-queue will stay at state $(0,0)$ forever.

For the above simplified QBD process, its transition matrix $\mathbf{P_3}$ can be determined based on (6) by setting the corresponding sub-matrices as follows:

For $M=1$,

$$\mathbf{B_0}=\mathbf{0}, \tag{D.1}$$
$$\mathbf{B_1}=[1], \tag{D.2}$$
$$\mathbf{B_2}=\mathbf{c}, \tag{D.3}$$
$$\mathbf{A_M}=\mathbf{Q}. \tag{D.4}$$

For $M\geqslant 2$,

$$\mathbf{B_0}=\mathbf{0}, \tag{D.5}$$
$$\mathbf{B_1}=[1], \tag{D.6}$$
$$\mathbf{B_2}=\mathbf{c}, \tag{D.7}$$
$$\mathbf{A_0}=\mathbf{0}, \tag{D.8}$$
$$\mathbf{A_1}=\mathbf{Q}, \tag{D.9}$$
$$\mathbf{A_2}=\mathbf{c}\cdot\mathbf{r}, \tag{D.10}$$
$$\mathbf{A_M}=\mathbf{Q}. \tag{D.11}$$

By rearranging $\mathbf{P_3}$ as

$$\mathbf{P_3} = \begin{bmatrix} 1 & \mathbf{0} \\ \mathbf{c}^+ & \mathbf{T} \end{bmatrix}, \tag{D.12}$$

we can see that matrices $\mathbf{c}^+$ and $\mathbf{T}$ are determined as (60)–(63). With matrices $\mathbf{c}^+$, $\mathbf{T}$ and π^*_Ω, the probability mass function (56) and CDF (57) of the source delay follow directly from the theory of Phase-type distribution [20].

Based on the probability mass function (56), the mean $\overline{U}$ of the source delay can be calculated by

$$\overline{U} = \sum_{u=1}^{\infty} u \cdot Pr\{U = u\} = \sum_{u=1}^{\infty} u\pi^-_\Omega \mathbf{T}^{u-1}\mathbf{c}^+$$

$$= \pi^-_\Omega \left(\sum_{u=1}^{\infty} u\mathbf{T}^{u-1} \right) \mathbf{c}^+ \tag{D.13}$$

Let

$$f(\mathbf{T}) = \sum_{u=1}^{\infty} u\mathbf{T}^{u-1}, \tag{D.14}$$

and use $f(x)$ to denote its corresponding numerical series

$$f(x) = \sum_{u=1}^{\infty} ux^{u-1} \tag{D.15}$$

$$= (1-x)^{-2}, \quad \text{for} \quad x < 1. \tag{D.16}$$

Since above simplified QBD process is actually an absorbing Markov Chain with transition matrix $\mathbf{P_3}$, we know from Theorem 11.3 in [38] that

$$\lim_{k\to\infty} \mathbf{T}^k = \mathbf{0}. \tag{D.17}$$

Based on the property (D.17) and the Theorem 5.6.12 in [39], we can see that the spectral radius $\rho(\mathbf{T})$ of matrix $\mathbf{T}$ satisfies following condition

$$\rho(\mathbf{T}) < 1. \tag{D.18}$$

From (D.14), (D.16) and (D.18), it follows that the matrix series $f(\mathbf{T})$ converge as

$$f(\mathbf{T}) = \lim_{g\to\infty} \sum_{u=1}^{g} u\mathbf{T}^{u-1} \tag{D.19}$$

$$= (\mathbf{I} - \mathbf{T})^{-2} \tag{D.20}$$

After substituting (D.20) into (D.13) and (58) then follows.

The derivation of the variance of source delay (59) could be conducted in a similar way and thus is omitted here.

References

[1] J. Andrews, S. Shakkottai, R. Heath, N. Jindal, M. Haenggi, R. Berry, D. Guo, M.J. Neely, S. Weber, S. Jafar, A. Yener, Rethinking information theory for mobile ad hoc networks, IEEE Commun. Mag. 46 (12) (2008) 94–101.

[2] A. Goldsmith, M. Effros, R. Koetter, M. MTdard, L. Zheng, Beyond Shannon: the quest for fundamental performance limits of wireless ad hoc networks, IEEE Commun. Mag. 49 (5) (2011) 195–205.

[3] L. Hanzo II, R. Tafazolli, A survey of QoS routing solutions for mobile ad hoc networks, IEEE Commun. Surv. Tutor. 9 (2) (2007) 50–70.

[4] L. Chen, W.B. Heinzelman, A survey of routing protocols that support QoS in mobile ad hoc networks, IEEE Network 21 (6) (2007) 30–38.

[5] M. Grossglauser, D.N. Tse, Mobility increases the capacity of ad hoc wireless networks, IEEE/ACM Trans. Network. 10 (4) (2002) 477–486.

[6] M.J. Neely, E. Modiano, Capacity and delay tradeoffs for ad-hoc mobile networks, IEEE Trans. Inform. Theory 51 (6) (2005) 1917–1936.

[7] J. Gao, X. Jiang, Delay modeling for broadcast-based two-hop relay MANETs, in: 11th International Symposium on Modeling and Optimization in Mobile, Ad Hoc, and Wireless Networks (WiOpt), 2013.

[8] A.E. Gamal, J. Mammen, B. Prabhakar, D. Shah, Optimal throughput-delay scaling in wireless networks – Part I: The fluid model, IEEE Trans. Inform. Theory 52 (6) (2006) 2568–2592.

[9] G. Sharma, R. Mazumdar, N.B. Shroff, Delay and capacity trade-offs for mobile ad hoc networks: a global perspective, IEEE/ACM Trans. Network. 15 (5) (2007) 981–992.

[10] D. Ciullo, V. Martina, M. Garetto, E. Leonardi, Impact of correlated mobility on delay-throughput performance in mobile ad hoc networks, IEEE/ACM Trans. Network. 19 (6) (2011) 1745–1758.

[11] P. Li, Y. Fang, J. Li, X. Huang, Smooth trade-offs between throughput and delay in mobile ad hoc networks, IEEE Trans. Mobile Comput. 11 (3) (2012) 427–438.

[12] J. Liu, X. Jiang, H. Nishiyama, N. Kato, Generalized two-hop relay for flexible delay control in MANETs, IEEE/ACM Trans. Network. 20 (6) (2012) 1950–1963.

[13] J. Liu, J. Gao, X. Jiang, H. Nishiyama, N. Kato, Capacity and delay of probing-based two-hop relay in MANETs, IEEE Trans. Wireless Commun. 11 (11) (2012) 4172–4183.

[14] P. Gupta, P. Kumar, The capacity of wireless networks, IEEE Trans. Inform. Theory 46 (2) (2000) 388–404.

[15] S.R. Kulkarni, P. Viswanath, A deterministic approach to throughput scaling in wireless networks, IEEE Trans. Inform. Theory 50 (6) (2004) 1041–1049.

[16] J. Liu, X. Jiang, H. Nishiyama, N. Kato, Delay and capacity in ad hoc mobile networks with f-cast relay algorithms, IEEE Trans. Wireless Commun. 10 (8) (2011) 2738–2751.

[17] R.P. Liu, G.J. Sutton, I.B. Collings, A new queueing model for QoS analysis of IEEE 802.11 DCF with finite buffer and load, IEEE Trans. Wireless Commun. 9 (8) (2010) 2664–2675.

[18] T. Small, Z. Hass, Resource and performance tradeoffs in delay-tolerant wireless networks, in: Proc. ACM SIGCOMM Workshop on Delay-Tolerant Networking (WDTN), 2005, pp. 260–267.

[19] B. Williams, T. Camp, Comparison of broadcasting techniques for mobile ad hoc networks, in: MobiHoc, 2002.

[20] G. Latouche, V. Ramaswamy, Introduction to matrix analytic methods in stochastic modeling, ASA–SIAM Series on Statistics and Applied Probability, 1999.

[21] C++ simulator for PD-f MANETs, 2013 <http://researchplatform.blogspot.jp/>.

[22] A.A. Hanbali, P. Nain, E. Altman, Performance of ad hoc networks with two-hop relay routing and limited packet lifetime (extended version), Perform. Eval. 65 (6–7) (2008) 463–483.

[23] A. Panagakis, A. Vaios, I. Stavrakakis, Study of two-hop message spreading in DTNs, in: WiOpt, 2007.

[24] M. Ibrahim, A.A. Hanbali, P. Nain, Delay and resource analysis in MANETs in presence of throwboxes, Perform. Eval. 64 (9–12) (2007) 933–947.

[25] R. Groenevelt, P. Nain, G. Koole, The message delay in mobile ad hoc networks, Perform. Eval. 62 (1–4) (2005) 210–228.

[26] A.A. Hanbali, A.A. Kherani, P. Nain, Simple models for the performance evaluation of a class of two-hop relay protocols, in: Proc. IFIP Networking, 2007, pp. 191–202.

[27] T. Spyropoulos, K. Psounis, C.S. Raghavendra, Efficient routing in intermittently connected mobile networks: the multiple-copy case, IEEE/ACM Trans. Network. 16 (1) (2008) 77–90.

[28] F. Baccelli, B. Blaszczyszyn, A new phase transitions for local delays in MANETs, in: INFOCOM, 2010.

[29] M. Haenggi, The local delay in poisson networks, IEEE Trans. Inform. Theory 59 (3) (2013) 1788–1802.

[30] Z. Gong, M. Haenggi, The local delay in mobile poisson networks, IEEE Trans. Wireless Commun. 12 (9) (2013) 4766–4777.

[31] J. Liu, X. Jiang, H. Nishiyama, N. Kato, X. Shen, End-to-end delay in mobile ad hoc networks with generalized transmission range and limited packet redundancy, in: WCNC, 2012c.

[32] B. Blaszczyszyn, P. Muhlethaler, Stochastic Analytic Evaluation of End-to-End Performance of Linear Nearest Neighbour Routing in MANETs with Aloha, Technical Report <http://arxiv.org/abs/1207.7219>.

[33] P. Nain, D. Towsley, A. Bar-Noy, P. Basu, M.P. Johnson, F. Yu, Estimating end-to-end delays under changing conditions, in: ACM MobiCom Workshop on Challenged Networks (CHANTS), 2013.

[34] F. Ciucu, O. Hohlfeld, P. Hui, Non-asymptotic throughput and delay distributions in multi-hop wireless networks, in: Annual Allerton Conference on Communication, Control, and Computing (Allerton), 2010.
[35] F. Ciucu, Non-asymptotic capacity and delay analysis of mobile wireless networks, in: SIGMETRICS, 2011.
[36] A.A. Hanbali, R. de Haan, R.J. Boucherie, J.-K. van Ommeren, Delay in a tandem queueing model with mobile queues: an analytical approximation, Probab. Eng. Inform. Sci. 28 (03) (2014) 363–387.
[37] A. Jindal, K. Psounis, Contention-aware performance analysis of mobility-assisted routing, IEEE Trans. Mobile Comput. 8 (2) (2009) 145–161.
[38] C.M. Grinstead, J.L. Snell, Introduction to Probability, second revised ed., American Mathematical Society, 1997.
[39] R.A. Horn, C.R. Johnson, Matrix Analysis, Cambridge University Press, 1990.

Juntao Gao received his B.S. and M.S. degrees both in Computer Science from Xidian University, Xi'an, China, in 2008 and 2010, respectively, and received his Ph.D. degree from Graduate School of Systems Information Science at Future University Hakodate, Japan, in 2014. He is an assistant professor at Graduate School of Information Science at Nara Institute of Science and Technology, Japan. His research interests are in the areas of performance modeling and analysis, stochastic optimization and control in wireless networks, queueing theory and its applications.

Yulong Shen received the B.S. and M.S. degrees in Computer Science and Ph.D. degree in Cryptography from Xidian University, Xi'an, China, in 2002, 2005, and 2008, respectively. He is currently an associate Professor at the School of Computer Science and Technology, Xidian University, China. He is also associate director of the Shaanxi Key Laboratory of Network and System Security and a member of the State Key Laboratory of Integrated Services networks Xidian University, China. He has also served on the technical program committees of several international conferences, including ICEBE, INCoS, CIS and SOWN. He is an IEEE and ACM member. Hiss research interest is wireless network security.

Xiaohong Jiang received his B.S., M.S. and Ph.D. degrees all from Xidian University, China. He is currently a full professor of Future University Hakodate, Japan. He was an Associate professor of Tohoku University, Japan, from February 2005 to March 2010, an assistant professor in Japan Advanced Institute of Science and Technology (JAIST), from October 2001 to January 2005. He was a JSPS research fellow at JAIST from October 1999 to October 2001. He was a research associate in the University of Edinburgh from March 1999 to October 1999. His research interests include computer communications networks, mainly wireless networks, optical networks, etc. He has published over 200 technical papers at premium international journals and conferences, which include over 20 papers published in IEEE journals like IEEE/ACM Transactions on Networking, IEEE Journal of Selected Areas on Communications, etc. He was the winner of the Best Paper Award and Outstanding Paper Award of IEEE WCNC 2012, IEEE WCNC 2008, IEEE ICC 2005-Optical Networking Symposium, and IEEE/IEICE HPSR 2002. He is a Senior Member of IEEE and a member of IEICE.

Jie Li received the B.E. degree in computer science from Zhejiang University, Hangzhou, China, the M.E. degree in Electronic Engineering and Communication Systems from China Academy of Posts and Telecommunications, Beijing, China. He received the Dr. Eng. degree from the University of Electro-Communications, Tokyo, Japan. He has been with University of Tsukuba, Japan, where he is a full Professor. His research interests are in mobile distributed multimedia computing and networking, OS, network security, modeling and performance evaluation of information systems. He received the best paper award from IEEE NAECON'97. He is a senior member of IEEE and ACM, and a member of IPSJ (Information Processing Society of Japan). He has served as a secretary for Study Group on System Evaluation of IPSJ and on several editorial boards for IPSJ Journal and so on, and on Steering Committees of the SIG of System EVAluation (EVA) of IPSJ, the SIG of DataBase System (DBS) of IPSJ, and the SIG of MoBiLe computing and ubiquitous communications of IPSJ. He has been a co-chair of several international symposia and workshops. He has also served on the program committees for several international conferences such as IEEE ICDCS, IEEE INFOCOM, IEEE GLOBECOM, and IEEE MASS.